

## Local structural variations near twins in $\text{YBa}_2\text{Cu}_3\text{O}_{7-\delta}$

G. P. E. M. van Bakel, P. A. Hof, J. P. M. van Engelen, P. M. Bronsveld, and J. Th. M. De Hosson  
*Department of Applied Physics, Materials Science Centre, University of Groningen, Nijenborgh 18,  
 9747 AG Groningen, The Netherlands*

(Received 28 December 1989)

Field-ion microscopic images of twinned high- $T_c$   $\text{YBa}_2\text{Cu}_3\text{O}_{7-\delta}$  revealed the characteristic fingerprint pattern combined with planar defects crossing the tip apex. The orientation and location of the twin boundaries was examined by transmission electron microscopy. Computed images revealed little twin-boundary contrast. Therefore, the observed boundary should be accounted for by other than a pure-crystallographic twin description, such as substructural variations or compositional disorder.

### INTRODUCTION

The new generation of high-critical-temperature superconductors, based on  $\text{YBa}_2\text{Cu}_3\text{O}_{7-\delta}$ , are known to exhibit relatively low critical current densities. For random polycrystalline bulk material the current density is on the order of  $10^3 \text{ A cm}^{-2}$  whereas in high-quality thin-film materials the current appears to be several orders of magnitude larger.<sup>1</sup> It is generally agreed that in these bulk materials there exists granular superconductivity in which the superconducting material with low dimensionality is coupled through weak-link regions separating one (sub)grain from another. Some measurements even suggest that these oxides may be in the superconducting glassy state which is attributed to inhomogeneities in the microstructure.<sup>2,3</sup> Consequentially, beside investigations on the electronic properties of these materials, research on the possible effects that substructural variations may have on the superconducting properties is of interest.

A prominent substructural feature is the formation of twins parallel to  $(1\bar{1}0)$  and  $(110)$ , which are formed to accommodate the shape change during the transformation from tetragonal to orthorhombic at about  $700^\circ\text{C}$ .<sup>4,5</sup> The projection of the atomic configuration along  $[001]$  direction is shown in Fig. 1. As a matter of course, this is an idealized picture in which oxygen-oxygen pairs together with vacancy-vacancy pairs are created across the interface and the Cu atoms are located right on the boundary itself. In the ideal case the twin structure can be associated with the switching of vacancy-Cu-vacancy and O-Cu-O chains across the boundary, producing a  $90^\circ$  configuration of the  $a$  and  $b$  axes. In fact, the twinning plane acts as an antiphase boundary plane for the vacancy-oxygen sublattice. In a more realistic picture, however, the Cu, O and vacancies may be redistributed near the interface that in turn affects the low dimensionality of the superconducting current along the Cu-O chains.

In this paper we concentrate on these structural variations across a twin boundary by using a field-ion microscope as a powerful tool.<sup>6</sup> In addition, transmission electron microscopy has been applied to inspect the field-ion microscopic-tip specimen and to investigate the twin-boundary configuration in the orthorhombic high- $T_c$  phase as well.

In a field-ion microscope, a sharp needle of the material

under investigation is subjected to a high electric voltage in the presence of an imaging gas ( $\text{He}, \text{Ne}, \text{Ar}, \text{H}_2$ ). Ionization of image gas atoms takes place preferentially at regions of high electric field, i.e., protruding atoms. At elevated voltages, surface atoms field evaporate from the apex.

Various attempts have been made to image  $\text{YBa}_2\text{Cu}_3\text{O}_{7-\delta}$  in the field-ion microscope.<sup>7</sup> This resulted in "fingerprint" patterns in most of the cases. Unfortunately, almost all conventional transmission electron microscopy (CTEM) micrographs shown in the literature<sup>8-10</sup> reveal the normal of the twin-plane oriented almost parallel to the tip axis. Computer simulations showed that either the Y or the Cu-O end planes are responsible for the observed pattern.<sup>7</sup> However, a nonspherical apex shape also contributes to the streaking.<sup>11</sup>

### PREPARATION OF HIGH- $T_c$ $\text{YBa}_2\text{Cu}_3\text{O}_{7-\delta}$

The method of preparation of the orthorhombic phase is described elsewhere<sup>12</sup> and is not different from conven-

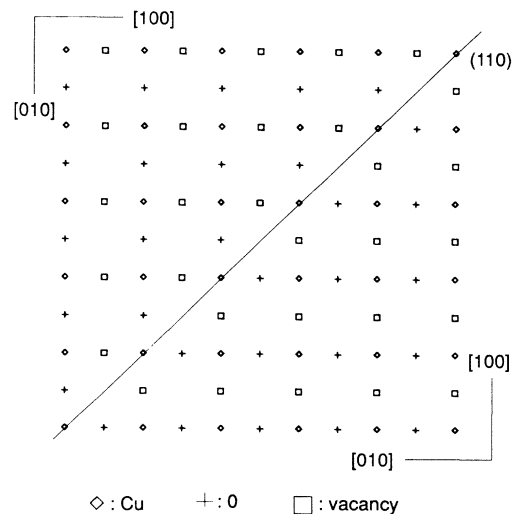


FIG. 1. Schematic model for a  $(110)$  twin interface of orthorhombic  $\text{YBa}_2\text{Cu}_3\text{O}_{7-\delta}$ .

tional methods. The porosity of the samples was as low as 20%. The chemical composition was checked by scanning electron microscopy and energy-dispersive spectrometry. X-ray diffraction showed the peak splitting which is characteristic for the orthorhombic phase. Electrical-resistance measurements reveal a  $T_c$  of 90 K. In order to obtain field emitter tips with appropriate apex radius (<100 nm), rods were isolated from the bulk material and electropolished in a solution of 10% perchloric acid in 2-butoxy-ethanol using 5 V dc resulting in tips with the required apex radius.

### MICROSCOPIC OBSERVATIONS

Few of the as-polished emitter tips showed acceptable apex shapes, considering the aspect ratio. Twin boundaries were observed by TEM in almost all of the inspected emitter tips, however, only a few exhibited the twin plane normal oriented perpendicular to the tip axis. This orientation is especially suitable because an intersection of the twin plane with the tip apex will persist during field evaporation.

At various stages of field-ion microscopic imaging TEM

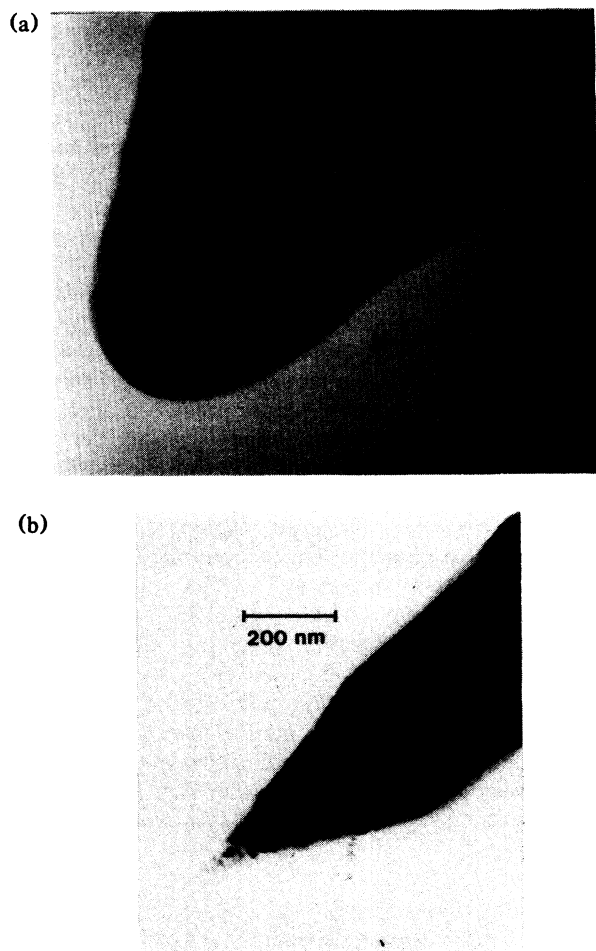


FIG. 2. TEM micrographs of emitter tip ( $c$  axis normal to plane). (a) Before field-ion microscopic imaging. (b) After field evaporation.

micrographs were taken which indicated that field evaporation took place. A typical example is shown in Fig. 2. The intersection of a twin boundary with the apex is clearly visible. The electron-diffraction patterns of the apex region under rotation of the tip with respect to the tip axis show the  $c$  axis to be normal to the tip axis [Fig. 3(a)]. The orientation of the [001] diffraction pattern with respect to the tip axis reveals the direction of the  $a$  and  $b$  axes. This is illustrated schematically in Fig. 3(b).

The emitter tips, inspected by CTEM, were subjected to field-ion microscopic imaging, the result of which is shown in Fig. 4. A line at which disordering takes place is also depicted in Fig. 4. Hydrogen was used as imaging gas. The characteristic fingerprint pattern, extensively reported in the literature,<sup>7</sup> developed at temperatures below 40 K. At higher temperatures (80 K), the images obtained were of an unstable nature. This is probably due to the higher residual gas pressure and mobility of adsorbates at the surface at elevated temperatures. The distance between spot arrays corresponds well to the  $c$  parameter of the orthorhombic phase (1.165 nm).

### DISCUSSION

The interpretation of field-ion images obtained can be facilitated by employing computer simulation techniques

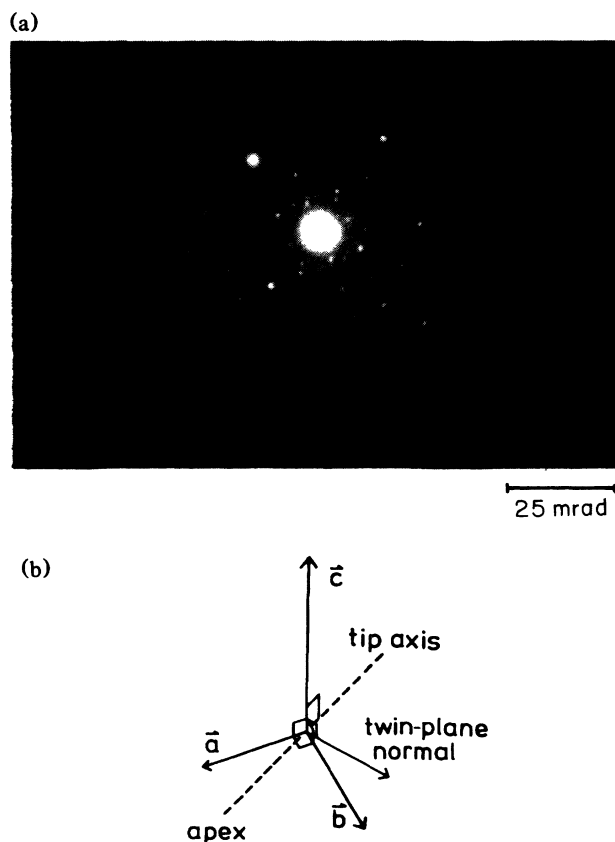


FIG. 3. (a) Selected-area electron-diffraction photograph of emitter tip, 200 kV, corresponding to Fig. 2(a). (b) Orientation of lattice vectors and twin plane in tip field-ion micrographs of emitter tip.

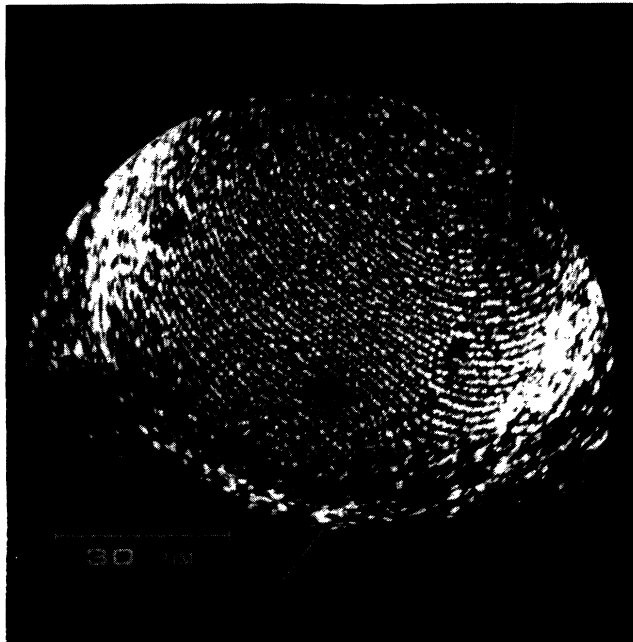


FIG. 4. Field-ion micrographs of emitter tip 10.1 kV, H<sub>2</sub>, 30 K.

of the images. In the simulations it is assumed that the tip possesses an atomically smooth surface and that the ionization probability near the surface is directly related to the protrusion of the surface atom. Only atoms lying within a thin spherical shell are supposed to be imaged<sup>13</sup> and are projected on a flat screen using a point projection. The model does not take into account local variations of the radius of curvature which result in a nonuniform electric field around the tip in reality. Computed images of twinned orthorhombic YBa<sub>2</sub>Cu<sub>3</sub>O<sub>7- $\delta$</sub>  were calculated using an algorithm that takes into account the nonspherical end form of the tip apex and the twinning. The tip shape and radius, the crystal orientation, and the location of the twin boundary were derived from the TEM observations. Different kinds of atoms were taken to be imaged, i.e., different locations in the unit cell, so as to compare the experimental and computed field-ion micrograph. This may facilitate the identification of the atom species in real images. Because the distance between the experimentally observed striped pattern corresponds well with the lattice parameter  $c$  in the [001] direction (1.165 nm) only two atomic layers are the possible source: the Cu-O planes between two Ba atoms or the planes containing Y atoms. There has been some debate in the literature about this pattern since the stripes were observed sometimes mainly in images taken from materials in the orthorhombic phase;<sup>7</sup> other reports mention that the pattern appears in both the orthorhombic and the tetragonal phase.<sup>9,14</sup> Upon aging, the stripes seem to become less distinct suggesting that Cu-O planes are actually imaged. When the superconductivity in the orthorhombic phase occurs in these Cu-O planes the striped pattern can be explained by the fact that in these planes the charge mobility results in the greatest electron depletion near the surface. As a conse-

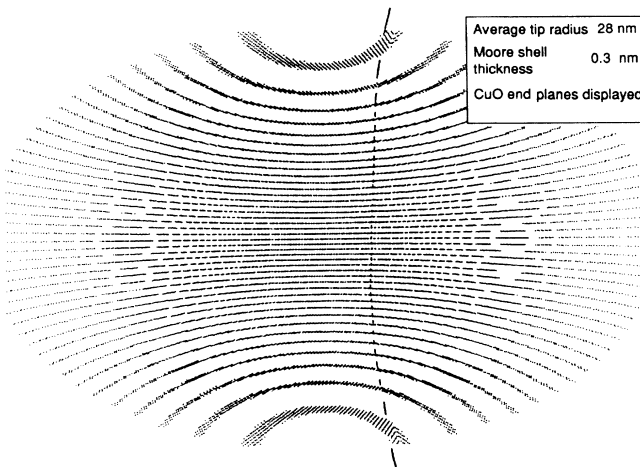


FIG. 5. Computed field-ion micrographs, orientation according to Fig. 3(b), apex shape corresponding to Fig. 2(b).

quence, these atoms are preferentially imaged.

In Fig. 5 a computed field-ion micrograph is depicted taking the Cu-O end planes being imaged. From the simulations the twin boundary is hardly detectable. Assuming a perfect crystallographic twin, only a small deviation is expected since the sublattices have nearly equal  $a$  and  $b$  lattice parameters ( $a = 0.382$  nm and  $b = 0.389$  nm,  $\Delta a/a \approx 2\%$ ). This is in contrast to the experimentally observed twin-boundary structure indicating a considerable width (Fig. 4) pointing at a variation of the oxygen-vacancy ordering across a twin boundary. This is in agreement with microscopic observations of the twin spacing<sup>15</sup> indicating that there does not exist a simple relationship between the twin spacing and  $(\Delta a/a)^{-1}$ . The variations in twin spacing means a variation in  $\Delta a/a$  and therefore in the oxygen ordering and in the strain along individual twins. Further, a simple model of the order-disorder transition in the Cu-O vacancy planes predict in all cases a depletion of oxygen at the twin-boundary region.<sup>16,17</sup>

Indeed, field-ion micrographs indicate as well that there exists an oxygen concentration profile across the twin boundary. In case of a crystallographic perfect twin boundary, the linear chains of Cu-O along the  $b$  direction which are believed to be necessary for 90-K superconductivity, zigzag through the  $a$ - $b$  plane with nearly 90% kinks at the twin boundary. In reality, substantial depletion of oxygen may exist near twin boundaries as suggested by these field-ion micrographs, that will affect the critical current densities. So, although claims have been made that superconductivity may be localized near twin boundaries, the above analysis suggests rather that twin boundaries may act as insulating layers because of the lack of oxygen ordering.<sup>18</sup>

## CONCLUSIONS

Twin boundaries in orthorhombic YBa<sub>2</sub>Cu<sub>3</sub>O<sub>7- $\delta$</sub>  observed by TEM are clearly visible in field-ion micrographs. They are far more prominent than computed im-

ages from unrelaxed twinned material show. This leads to our conclusion that the twin-boundary region deviates from the crystallographic description. This deviation could be accounted for by regional structural and/or compositional disordering suggesting that twin boundaries may act as insulating layers because of the lack of oxygen ordering.

#### ACKNOWLEDGMENTS

This work is part of the research program of the Foundation for Fundamental Research on Matter (FOM-Utrecht) and has been made possible by financial support from the Netherlands Organization for Research (NWO-The Hague).

- 
- <sup>1</sup>R. J. Cava, B. Batlogg, R. B. van Dover, D. W. Murphy, T. Siegrist, J. P. Remeika, E. A. Rietman, S. Zahurak, and G. P. Espinosa, *Phys. Rev. Lett.* **58**, 1676 (1987).
- <sup>2</sup>J. Bardeen, in *Proceedings of the International Workshop on Novel Mechanisms of Superconductivity*, edited by Z. Kresin and S. A. Wolf (Plenum, New York, 1987).
- <sup>3</sup>G. Deutscher and K. A. Müller, *Phys. Rev. Lett.* **59**, 1745 (1987).
- <sup>4</sup>G. van Tendeloo, H. W. Zandbergen, and S. Amelinckx, *Solid State Commun.* **63**, 603 (1987).
- <sup>5</sup>M. Hervieu, B. Domenges, C. Michel, G. Heger, J. Provost, and B. Raveau, *Phys. Rev. B* **36**, 3920 (1987).
- <sup>6</sup>E. W. Müller and T. T. Tsong, *Field Ion Microscopy Principles and Applications* (Elsevier, New York, 1968).
- <sup>7</sup>A. J. Melmed, R. D. Shull, C. K. Chiang, and H. A. Fowler, *Mater. Sci. Eng.* **100**, L27 (1988).
- <sup>8</sup>G. L. Kellogg and S. S. Brenner, *Appl. Phys. Lett.* **51**, 1851 (1987).
- <sup>9</sup>G. L. Kellogg and S. S. Brenner, *J. Phys. (Paris) Colloq.* **49**, C6-465 (1988).
- <sup>10</sup>G. Zaharchuk, L. von Alvensleben, M. Oehring, and P. Haasen, *J. Phys. (Paris) Colloq.* **49**, C6-471 (1988).
- <sup>11</sup>H. B. Elswijk, A. J. Melmed, and H. A. Fowler, *J. Phys. (Paris) Colloq.* **49**, C6-489 (1988).
- <sup>12</sup>J. M. Tarascon, P. B. Barboux, B. G. Bagley, L. H. Greene, and G. W. Hull, *Mater. Sci. Eng. B* **1**, 29 (1988).
- <sup>13</sup>A. J. W. Moore, *Phys. Chem. Solids* **23**, 907 (1962).
- <sup>14</sup>A. J. Melmed, R. D. Shull, and C. K. Chiang, *J. Phys. (Paris) Colloq.* **49**, C6-459 (1988).
- <sup>15</sup>M. Sarikaya, R. Kikuchi, and I. A. Aksay, *Physica C* **152**, 161 (1988).
- <sup>16</sup>A. Rohledo and C. Varea, *Phys. Rev. B* **37**, 631 (1988).
- <sup>17</sup>M. Sarikaya and E. A. Stern, *Phys. Rev. B* **37**, 9373 (1988).
- <sup>18</sup>M. M. Fang, V. G. Kogan, D. K. Finnemore, J. R. Chen, L. S. Chumbley, and D. E. Farrel, *Phys. Rev. B* **37**, 2334 (1988).

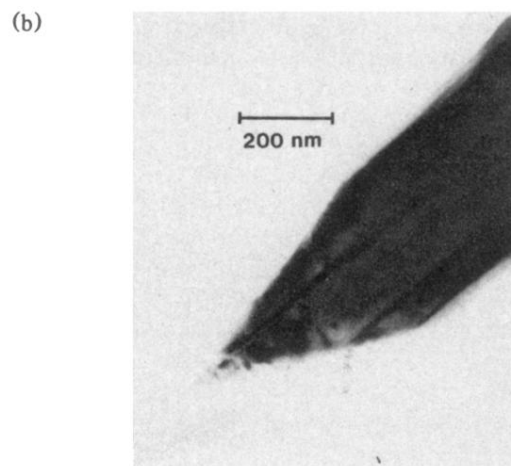
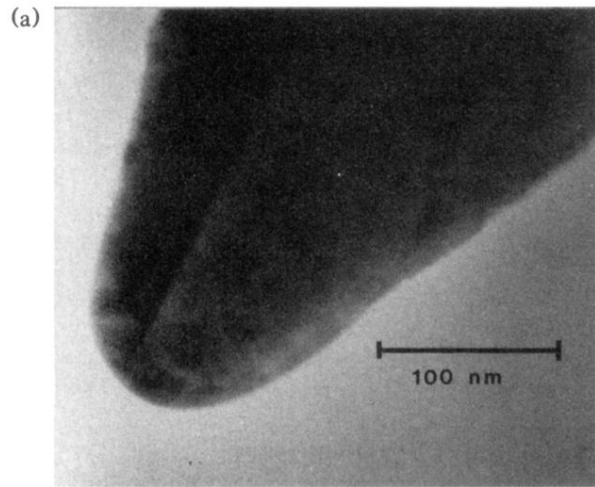


FIG. 2. TEM micrographs of emitter tip ( $c$  axis normal to plane). (a) Before field-ion microscopic imaging. (b) After field evaporation.

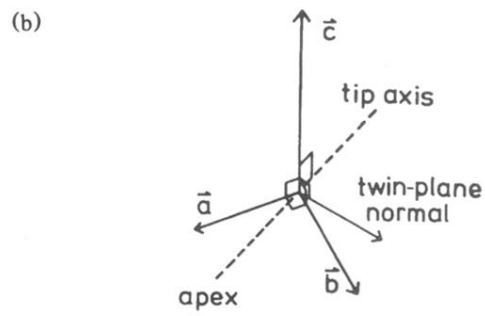
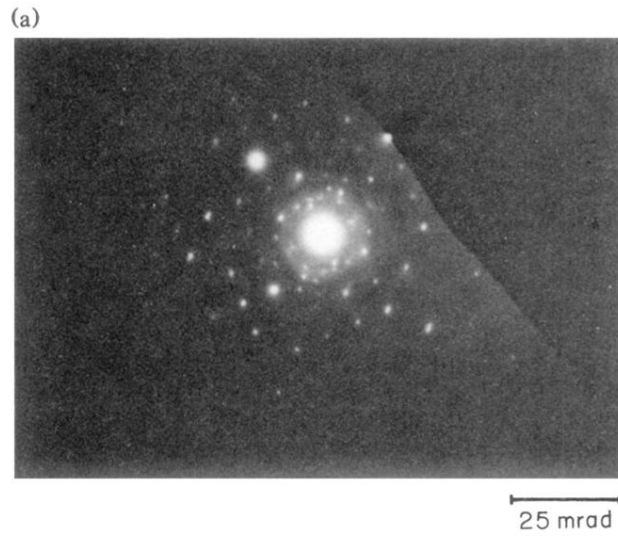


FIG. 3. (a) Selected-area electron-diffraction photograph of emitter tip, 200 kV, corresponding to Fig. 2(a). (b) Orientation of lattice vectors and twin plane in tip field-ion micrographs of emitter tip.

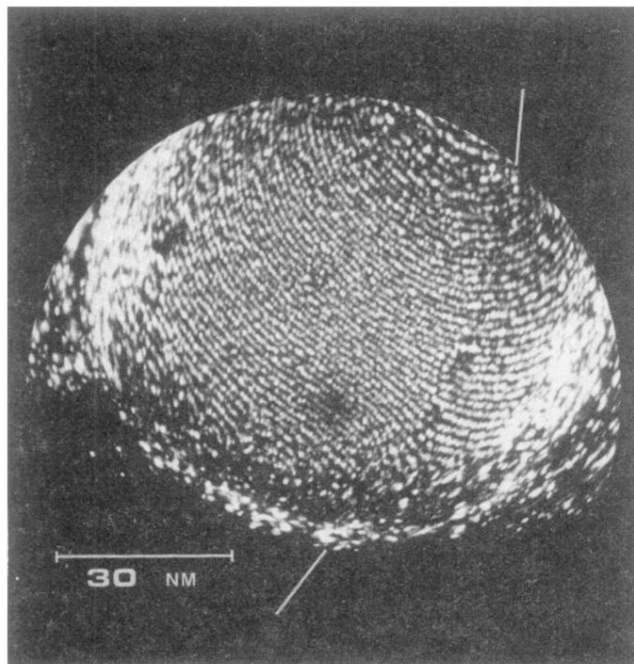


FIG. 4. Field-ion micrographs of emitter tip 10.1 kV, H<sub>2</sub>, 30 K.